Oncology Research, Vol. 27, pp. 1061–1068
Printed in the USA.

0965-0407/19 $90.00 + .00
DOI: https://doi.org/10.3727/096504019X15565325878380
E-ISSN 1555-3906
www.cognizantcommunication.com

miR-186 Suppresses the Progression of Cholangiocarcinoma Cells Through Inhibition of Twist1

Ming Zhang, Baochang Shi, and Kai Zhang

Department of Hepatobiliary Surgery, Shandong Provincial Third Hospital, Jinan, Shandong, P.R. China

Deregulation of miR-186 and Twist1 has been identified to be involved in the progression of multiple cancers. However, the detailed molecular mechanisms underlying miR-186-involved cholangiocarcinoma (CCA) are still unknown. In this study, we found that miR-186 was downregulated in CCA tissues and cell lines, and negatively correlated with the expression of Twist1 protein. In vitro assays demonstrated that miR-186 mimics repressed cell proliferation, in vivo tumor formation, and caused cell cycle arrest. miR-186 mimics also inhibited the migration and invasion of CCLP1 and SG-231 cells. Mechanistically, the 3′-untranslated region (3′-UTR) of Twist1 mRNA is a direct target of miR-186. Further, miR-186 inhibited the expressions of Twist1, N-cadherin, vimentin, and matrix metallopeptidase 9 (MMP9) proteins, whereas it increased the expression of E-cadherin in CCLP1 and SG-231 cells. Silencing of Twist1 expression enhanced the inhibitory effects of miR-186 on the proliferation, migration, and invasion of CCLP1 and SG-231 cells. In conclusion, miR-186 inhibited cell proliferation, migration, invasion, and epithelial–mesenchymal transition (EMT) through targeting Twist1 in human CCA. Thus, miR-186/Twist1 axis may benefit the development of therapies for CCA.

Key words: miR-186; Cholangiocarcinoma (CCA); Twist1; E-cadherin

INTRODUCTION

Bile duct cancer is one of the most aggressive cancers worldwide[1], which are characterized by rapid progression, metastasis, and lack of accurate diagnosis at an early stage[2]. Till now, cytotoxic chemotherapy remains the only therapeutic method for unresectable cholangiocarcinoma (CCA). Unfortunately, CCA resists most chemotherapy, and 5-year overall survival status is extremely poor, remaining at 10%[3,4]. To improve the diagnosis and prognosis of CCA patients, it is crucial to investigate molecular mechanisms to develop biological treatment.

MicroRNAs (miRNAs) are regulatory molecules involved in many diseases, which are small noncoding RNAs and negatively regulate gene expression through targeting the 3′-untranslated region (3′-UTR) of mRNAs[4]. miRNAs play key roles in numerous biological processes, including cell growth, cell cycle progression, apoptosis, migration, and invasion[5]. Aberrant expression of miR-186 has been found in the initiation and development of some tumors. Tian et al. reported that miR-186 is a regulator of cutaneous squamous cell carcinoma cell proliferation by directly targeting apoptotic protease activating factor-1[6]. Cao et al. suggested that miR-186 negatively regulates osteosarcoma cell survival and metastasis by targeting TBL1XR1[7]. Recently, increasing evidence indicated that Twist1 was deregulated in human tumors, such as colorectal cancer[8], lung adenocarcinoma[9], and ovarian carcinoma[10]. However, the expression and role of miR-186 and Twist1 in CCA have never been largely explored.

In the present study, we demonstrated that miR-186 was a tumor suppressor in CCA cells and a key regulator of Twist1 expression. In addition, the results revealed that miR-186-induced downregulation of Twist1 was associated with the inhibition of CCA cell proliferation, migration, and invasion. We then present evidence for the potential use of miR-186 targeting Twist1 for the treatment of CCA.

MATERIALS AND METHODS

Tissue Samples

Freshly resected tumor samples were collected from 60 patients with CCA who underwent complete surgical resection at Shandong Provincial Hospital (Jinan, Shandong, P.R. China) between March 2013 and December 2015. The demographics of 60 patients with CCA

Address correspondence to Kai Zhang, Department of Hepatobiliary Surgery, Shandong Provincial Third Hospital, No. 12, Central Wuying Hill Road, Jinan 250031, Shandong, P.R. China. E-mail: zhangkaislsy@163.com

Table 1. The Demographics of 60 Patients With Cholangiocarcinoma (CCA)

Characteristics	*N*
Age	
≥65	38
<65	22
Gender	
Male	35
Female	25
Tumor size (cm)	
≥5	39
<5	21
Histological types	
Adenocarcinoma	4
Squamous carcinoma	56
Location	
Intrahepatic	14
Extrahepatic	46
Lymph node metastasis	
Negative	32
Positive	28
TNM stage	
I–II	26
III–IV	34

are provided in Table 1. The disease status of the tissue samples was confirmed by at least two experienced pathologists. Patient follow-up was conducted routinely until February 2019, when the follow-up data were recorded and analyzed as described previously. The average follow-up time of the cohort was 26 months. The overall survival (OS) was defined as the time from the date of clinical diagnosis to the date of death from any cause. The recurrence-free survival (RFS) was defined as the time between the date of surgery to date of relapse or death. This study was approved by the Research Ethics Committee of Shandong Provincial Third Hospital. Written informed consent was acquired from all the patients. Tissue specimens were immediately frozen in liquid nitrogen after surgery and stored at −80°C until use.

Cell Culture

Human CCA cell lines CCLP1, SG-231, and human intrahepatic bile duct epithelial cell line HIBEC were purchased from Tianjin Sai'er Biotechnology Co. Ltd. (Tianjin, P.R. China). All CCA cells were cultured in RPMI-1640 medium (Thermo Fisher Scientific, Waltham, MA, USA) supplemented with 10% fetal bovine serum (FBS; Gibco, Carlsbad, CA, USA). HIBEC cells were cultured in Dulbecco's modified Eagle's medium (DMEM; Gibco Laboratories, Grand Island, NY, USA) with 10% fetal FBS (Gibco, Carlsbad, CA, USA). Cultures were maintained in a humidified atmosphere at 37°C with 5% CO_2.

Cell Transfection

miR-186 mimics and negative control miRNAs (miR-NC) were purchased from RiboBio (Guangzhou, P.R. China). Twist1-specific small interfering RNAs (si-Twist1) and control small interfering RNAs (si-control) were purchased from GeneChem (Shanghai, P.R. China). Cells were cultured to 80% confluence, followed by transfection with miR-186 mimics (50 nM) or control using Lipofectamine 2000 reagent (Thermo Fisher Scientific) according to the manufacturer's protocol. The cells were cultured in transfection media for 6 h, and then the media were replaced by complete medium for the following assays.

qRT-PCR Analysis

Total RNA was extracted from the cells or tissues using the miRNA isolation kit (Ambion, Austin, TX, USA). Reverse transcriptions were performed using an RNA PCR kit (Takara Bio, Otsu, Shiga, Japan) in accordance with the manufacturer's instructions. To quantify gene transcripts, real-time PCR was performed using SYBR-Green Premix Ex Taq (Takara Bio) on LightCycler 480 (Roche, Basel, Switzerland). U6 and glyceraldehyde-3-phosphate dehydrogenase (GAPDH) were used as the normalizing controls for quantifying miRNA and mRNA, respectively. For RT-PCR, the amplified PCR products were resolved by electrophoresis on 2% agarose gels and were visualized by ethidium bromide staining.

Western Blot Analysis

Tissues and cells were lysed using lysis buffer containing protease inhibitor cocktail (Thermo Fisher Scientific). The BCA Protein Assay kit (Pierce, Rockford, IL, USA) was used to detect the total concentration of protein. Protein extract (50 mg) was separated by sodium dodecyl sulfate-polyacrylamide gel electrophoresis (SDS-PAGE), and subsequently transferred onto polyvinylidene difluoride membranes (PVDF; EMD Millipore, Boston, MA, USA). The membranes were incubated with the appropriate primary antibodies or GAPDH (1:1,000; Santa Cruz Biotechnology, Santa Cruz, CA, USA) overnight at 4°C. Further, the membranes were incubated with anti-mouse or rabbit peroxidase-conjugated secondary antibodies (HRP; 1:5,000; Santa Cruz Biotechnology) for 1 h at room temperature. Proteins were visualized using an enhanced chemiluminescence system (Amersham Biosciences, Buckinghamshire, UK) and quantified using Image Lab Software version 4.1 (Bio-Rad, Hercules, CA, USA).

Cell Proliferation Assay

Cell Counting Kit-8 (CCK-8; Dojindo Molecular Technologies, Inc., Kumamoto, Japan) was used to assess cell viability. Cells (1×10^5) were seeded into a 96-well plate and incubated overnight in the previously described

conditions. Following this, the medium was removed, and the cells were washed three times with PBS. DMEM (90 µl) and CCK8 (10 µl) were subsequently added to each well and incubated for 1.5 h at 37°C; a microplate reader was used to measure the optical density (OD) at 450 nm.

Cell Cycle Analysis

Cells were washed twice with ice-cold PBS and resuspended in 1 ml of ice-cold 70% ethanol. After centrifugation, the cells were washed with ice-cold PBS and then resuspended with 200 µl of PBS and 20 µl of DNase-free Rnase A for 30 min at 37°C . They were then stained with 400 µl of a propidium iodide working solution. Cells were then analyzed with flow cytometry (Beckman Coulter, Fullerton, CA, USA) to determine the cell cycle distribution. The percentage of cells in each cell cycle stage (G_0/G_1, S, or G_2/M) was calculated using the WinCycle32 software.

Cell Migration and Invasion Assays

Cell migration assay was performed by Transwell chambers using 24-well plates with 8-µm pores (Corning Incorporated, Corning, NY, USA). Cells were starved in the serum-free DMEM for 12 h; 1×10^5 cells were seeded in the upper chamber after being resuspended in serum-free medium. The lower chambers were filled with DMEM plus 10% FBS. After 12 h of incubation at 37°C, migrated cells were fixed with 100% methanol and stained with 0.1% crystal violet. Ten random fields for each membrane were counted. The experimental procedures of invasion assay were similar to the migration assay except that the membrane was coated with Matrigel (Corning Incorporated); 2×10^5 cells were seeded in the upper chamber and the time of incubation extended to 24 h.

Luciferase Reporter Assay

Cells were inoculated into 24-well plates at a density of 2×10^4 cells/well and cultured for 24 h. Cells were then cotransfected with pmir-GLO-wide type (WT) or mutant (MUT) Twist1 3′-UTR reporter plasmids (100 ng) and miR-186 mimics/miR-NC (10, 20, 30, 40, and 50 nM). The firefly and *Renilla* luciferase activities were analyzed using the commercial Dual-Luciferase reporter assay system (Promega, Madison, WI, USA) on a microplate luminometer at 48 h after transfection, and the firefly luciferase activity was normalized to the *Renilla* luciferase activity.

Xenograft Mouse Models

All animal procedures were performed in accordance with the Care and Use of Laboratory Animals and protocols approved by the Animal Care Committee of Shandong Provincial Third Hospital (Jinan, Shandong, P.R. China). The BALB/c nude mice (Shandong University, Jinan, Shandong, P.R. China) were subcutaneously inoculated with transfected cells and corresponding control cells (2×10^6 cells/100 µl PBS/mouse) (four mice/group). Tumor growth in vivo was monitored by other investigators that were blinded to the group allocation. Tumor volume was measured with a caliper and calculated by the formula, tumor size $= ab^2/2$, where a is the larger of the two dimensions and b is the smaller. The tumor-bearing mice were sacrificed 4 weeks after tumor cell inoculation, and the xenografted tumors were then removed and weighed.

Statistical Analysis

Each experiment was performed in triplicate and repeated at least three times. Survival rates were constructed using the Kaplan–Meier method, and differences between survival curves were examined with the log rank test. Multivariate analysis was performed using the Cox proportional hazards model and a stepwise procedure. All the data were presented as means ± SD and treated for statistics analysis by GraphPad Prism 6.0 statistical software (GraphPad Software, Inc., San Diego, CA, USA). Comparison between groups was made using ANOVA, and statistically significant difference was defined as a value of $p < 0.05$.

RESULTS

miR-186 Is Downregulated and Twist1 Is Upregulated in CCA Tissues and Cells

In this study, the expressions of miR-186 and Twist1 in 60 paired CCA tissue specimens and cell lines were measured. The results of qRT-PCR revealed that the miR-186 expressions in CCA tissues were significantly decreased in contrast with that in the paired paracarcinoma tissues ($p < 0.001$) (Fig. 1A). On the contrary, Twist1 expressions in CCA tissues were found to be prominently upregulated ($p < 0.001$) (Fig. 1B). Additionally, the same result was also found in CCA cell lines. The results of qRT-PCR revealed a lower miR-186 expression in both CCLP1 and SG-231 cells than that in HIBEC ($p < 0.001$) (Fig. 1A). Subsequently, we also measured the Twist1 protein expression in CCA cell lines. The results demonstrated a significant decrease in CCLP1 and SG-231 cells compared with that in HIBEC (Fig. 1B). Moreover, to better understand the relationship between miR-186 and Twist1, we analyzed the correlation of miR-186 and Twist1 expression using Spearman's correlation analysis, and found a negative correlation ($R^2 = 0.646$; $p < 0.001$).

miR-186 and Twist1 Correlate With Poor Prognoses

According to the median level of miR-186 and Twist1 in CCA tissues as the cutoff, we divided all patients into high or low expression groups. We found that patients with low miR-186 expression had poorer

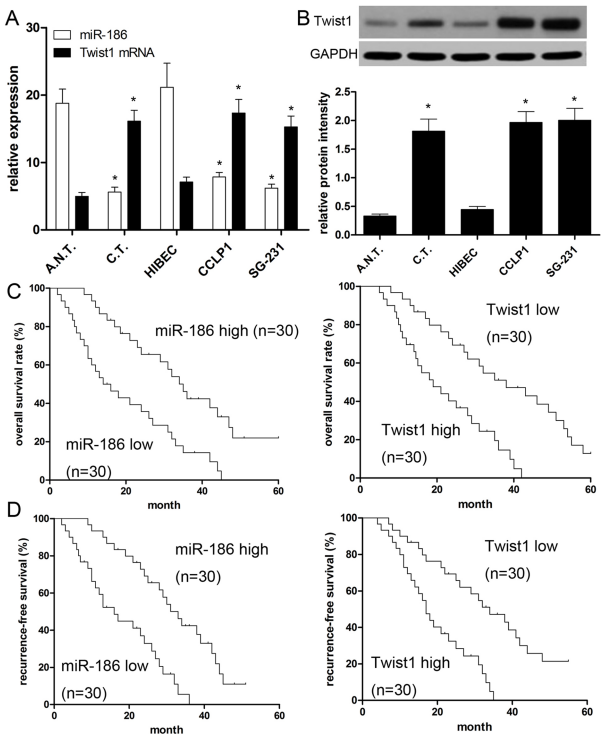

Figure 1. Expressions of miR-186 and Twist1 in cholangiocarcinoma (CCA) tissues and cell lines, and their associations with prognosis. (A) qRT-PCR was performed to measure the expression of miR-186 and Twist1 mRNA in CCA cells: 60 cases of cancer tissues (C.T.) and adjacent normal tissues (A.N.T.). The bands were measured by densitometry with Quantity One quantitation analysis software package. U6 and GAPDH were used for loading normalization. (B) Western blot was performed to measure the relative expression of Twist1 protein in human CCA tissues and cell lines (CCLP1 and SG-231) compared with normal tissues and human intrahepatic bile duct epithelial cell line HIBEC. (C) Kaplan–Meier plotter was employed to analyze overall survival (OS) of patient cohort; populations were divided by median value. (D) Kaplan–Meier plotter was employed to analyze regression-free survival (RFS) of patient cohort; populations were divided by median value. Data are presented as mean ± SD of at least three independent experiments. *$p < 0.001$ versus control.

overall survival than those with high miR-186 expression ($p = 0.0003$) (Fig. 1C). Likewise, patients with low miR-186 expression had poorer recurrence-free survival (RFS) ($p = 0.0001$) (Fig. 1D). Additionally we found that patients with high Twist1 protein expression had inferior overall survival (OS; $p = 0.0011$) and RFS ($p = 0.0015$) in comparison with those who had low Twist1 expression (Fig. 1C and D). As shown in Tables 2 and 3, univariate and multivariate Cox regression analysis revealed that miR-186 or Twist1 expression was strongly associated with OS and RFS ($p < 0.001$). These findings suggested that miR-186 or Twist1 can serve as an independent prognostic biomarker.

miR-186 Inhibits In Vitro Proliferation and In Vivo Tumor Formation

The present study restored miR-186 expression level in CCLP1 and SG-231 cells via transfection of miR-186 mimics or miR-NC, respectively. The results revealed that miR-186 mimics induced miR-186 expression levels in CCLP1 and SG-231 cells, respectively, compared with the negative control transfection ($p < 0.001$) (Fig. 2A). Following alteration of miR-186 expression level, CCLP1 and SG-231 cells were subjected to cell proliferation assays and flow cytometry. The CCK-8 assay revealed that miR-186 mimics reduced CCLP1 and SG-231 cell proliferation, compared with the miR-NC ($p < 0.001$) (Fig. 2B). Furthermore, we observed that miR-186 mimics in CCLP1 and SG-231 cells led to an accumulation of cells in the G_1 phase and a decrease in the number of cells in the S and G_2/M phases, indicating that miR-186 mimics resulted in a shift in the cell cycle distribution in CCLP1 and SG-231 cells ($p < 0.001$) (Fig. 2C). Subsequently, we investigated whether miR-186 was involved in in vivo tumor formation. We found that tumor size was effectively suppressed in miR-186 mimic-treated nude mice, compared with miR-NC ($p < 0.001$) (Fig. 2D). Moreover, miR-186 mimics led to a marked loss in tumor weight compared with miR-NC ($p < 0.001$) (Fig. 2E). These findings suggesting that miR-186 plays its anti-oncogenic role in cell proliferation.

miR-186 Suppresses Cell Migration and Invasion

In this work, we transfected miR-186 mimics into CCLP1 and SG-231 cells to investigate its role in CCA. First, we identified the expression level of miR-186 using qRT-PCR. Then Transwell assay was conducted to measure the migration and invasion abilities of transfected cells. We found that the migration and invasion abilities were reduced by miR-186 mimics in CCLP1 and SG-231 cells compared with their miR-NC groups ($p < 0.001$) (Fig. 3A and B). These results suggested that miR-186 functions as a suppressor, which exerts an inhibitory effect on cell migration and invasion in CCA. Further, miR-186 inhibited the expressions of N-cadherin and MMP9 proteins, whereas it increased the expression of E-cadherin in CCLP1 and SG-231 cells.

miR-186 Suppresses Twist1 Expression and EMT

EMT has been reported to play an important role in the progression and metastasis of cancer cells. However, the exact role of miR-186 in EMT of CCA cells has not yet been identified. In this study, we used Western blot to detect the expressions of relevant EMT biomarkers in CCLP1 and SG-231 cells. Our data also demonstrated a significant reduction in transcription factor Twist1 and mesenchymal phenotype markers such as N-cadherin, vimentin, and MMP9 in CCLP1 and SG-231 cells

Table 2. Univariate Analyses of Factors Associated With Overall Survival (OS) and Recurrence-Free Survival (RFS)

	OS		RFS	
Variable	HR (95% CI)	*p* Value	HR (95% CI)	*p* Value
Age	1.886 (0.626–5.684)	0.260	1.765 (0.661–4.716)	0.257
Gender	1.902 (0.696–5.198)	0.211	1.589 (0.911–2.773)	0.103
Tumor differentiation	1.148 (0.940–1.402)	0.175	1.219 (0.964–1.541)	0.098
Tumor size (≥5 cm vs. <5 cm)	1.731 (1.123–2.684)	**0.014**	1.275 (1.006–1.616)	**0.045**
Lymph node metastasis	2.150 (1.476–3.133)	**0.001**	2.601 (1.682–4.033)	**0.001**
Child–Pugh score (A vs. B)	1.203 (0.502–2.883)	0.674	1.501 (0.632–3.603)	0.399
TNM stage	2.864 (1.052–7.813)	**0.017**	2.414 (1.362–4.271)	**0.001**
CEA (≥5 ng/ml vs. <5 ng/ml)	2.008 (1.131–3.564)	**0.017**	2.257 (1.418–3.594)	**0.001**
miR-186 expression (high vs. low)	2.701 (1.651–4.411)	**<0.001**	2.572 (1.531–4.310)	**<0.001**
Twist1 expression (high vs. low)	2.624 (1.703–4.054)	**<0.001**	2.803 (1.412–5.561)	**<0.001**

CEA, carcinoembryonic antigen; HR, hazard ratio; 95% CI, 95% confidence interval. The bold values are considered to be significant differences.

Table 3. Multivariate Analyses of Factors Associated With OS and RFS

	OS		RFS	
Variables	HR (95% CI)	*p* Value	HR (95% CI)	*p* Value
Tumor size (≥5 cm vs. <5 cm)	1.271 (0.798–2.207)	0.313	NA	
Lymph node metastasis	1.858 (1.329–2.598)	**< 0.001**	1.486 (1.045–2.114)	**0.028**
TNM stage	1.314 (0.932–1.854)	0.119	1.270 (0.928–1.739)	0.136
CEA (≥5 ng/ml vs. <5 ng/ml)	1.183 (0.674–3.304)	0.222	NA	
miR-186 expression (high vs. low)	2.209 (1.301–3.752)	**0.002**	2.160 (1.329–3.510)	**0.001**
Twist1 expression (high vs. low)	2.244 (1.435–3.510)	**< 0.001**	2.013 (1.056–3.837)	**0.022**

CEA, carcinoembryonic antigen; HR, hazard ratio; 95% CI, 95% confidence interval; NA, not applicable. The bold values were considered to be significant differences.

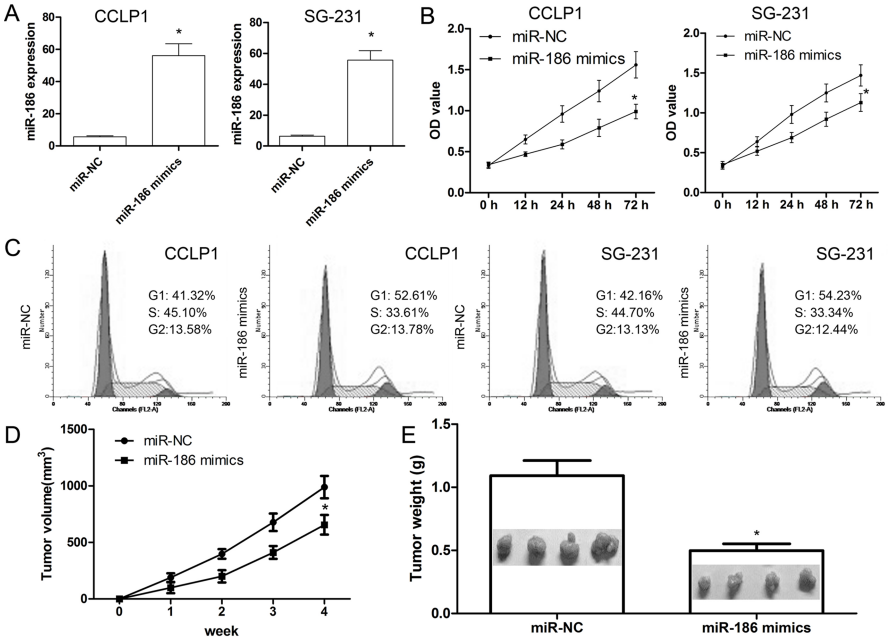

Figure 2. miR-186 suppresses cell proliferation and cell cycle. (A) CCLP1 and SG-231 cells were transiently transfected with miR-186 mimics or miR-NC, respectively. (B) CCK-8 assay was performed to detect cell proliferation. (C) Cell cycle was analyzed by flow cytometry at 72 h posttransfection. (D) Tumor size was measured every 7 days. (E) After 4 weeks, the mice were sacrificed, and tumors were imaged and weighed. Values presented as mean ± SD. *$p < 0.001$ versus control.

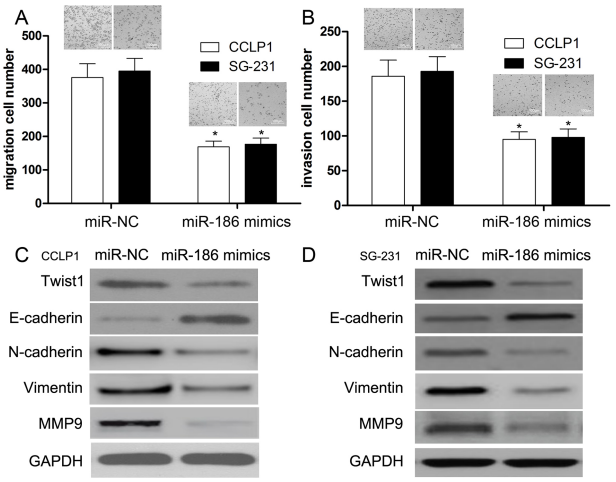

Figure 3. miR-186 inhibits the migration, invasion, and epithelial–mesenchymal transition (EMT) of CCA cells. Transwell assay was performed to determine the migration (A) and invasion (B) ability of CCLP1 and SG-231 cells. Representative images showed migrating and invasive cells in the lower chamber stained with crystal violet. (C) Expressions of Twist1, E-cadherin, N-cadherin, vimentin, and metallopeptidase 9 (MMP9) were measured by Western blotting in CCLP1 cells. (D) Expressions of Twist1, E-cadherin, N-cadherin, vimentin, and MMP9 were measured by Western blotting in SG-231 cells. Data of (A) and (B) are presented as mean ± SD of at least three independent experiments *$p < 0.001$ versus control.

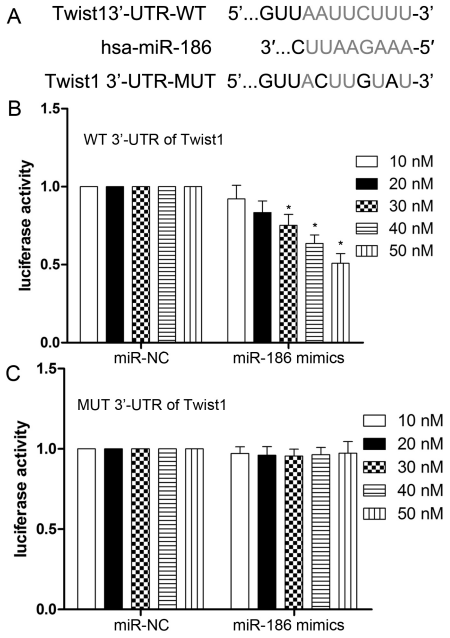

Figure 4. Twist1 3′-UTR is a direct target of miR-186. (A) A schematic shows reporter constructs of wild-type Twist1 3′-UTR and miR-186-binding sites. (B, C) HEK-293T cells were cotransfected with pmir-GLO-wide type (WT) or mutant (MUT) Twist1 3′-UTR reporter plasmids (100 ng) and miR-186 mimics/miR-NC (10, 20, 30, 40, and 50 nM). Relative luciferase activities of the wild type and mutant type were detected by fluorescent intensity. Values are presented as mean ± SD. *$p <$ 0.001 versus control.

($p < 0.01$) (Fig. 3C and D). Conversely, the expression of E-cadherin was obviously increased in miR-186 mimic-transfected CCLP1 and SG-231 cells ($p < 0.01$) (Fig. 3C and D), suggesting that miR-186 overexpression restored their epithelial phenotypes and inhibited EMT in CCLP1 and SG-231 cell lines.

Twist1 Is a Direct Target of miR-186

To elucidate the potential mechanism of miR-186 in suppressing cell proliferation, migration, and invasion, we searched for the potential target genes of miR-186 using the bioinformatics algorithm TargetScan (http://www.targetscan.org/vert_71/). Twist1, containing a potential binding site, was selected for experimental validation (Fig. 4A). Luciferase reporter assay showed that the luciferase activity was significantly reduced when HEK-293T cells were cotransfected with pmir-GLO-Twist1-3′-UTR (WT) and miR-186 ($p < 0.001$) (Fig. 4B). There was no effect on cells cotransfected with pmir-GLO-Twist1-3′-UTR (MUT) and miR-186 ($p > 0.05$) (Fig. 4C).

Twist1 Silencing Contributes to the Biological Functions of miR-186

Twist1 siRNA or negative control was transfected into CCLP1 and SG-231 cells to investigate the effect of Twist1. The expression of Twist1 decreased by si-Twist1 was validated by Western blot analysis (Fig. 5A). Then CCK-8 assay validated that knockdown of Twist1 significantly enhanced inhibitory effects of miR-186 overexpression on the proliferation of CCLP1 and SG-231 cells ($p < 0.001$) (Fig. 5B). Further, we observed that overexpression of miR-186 and knockdown of Twist1 remarkably significantly increased the proportion of cells in the G_1 phase and significantly decreased the proportion of cells in the G_2/M phase in CCLP1 and SG-231 cells compared with three other groups ($p < 0.001$) (Fig. 5C). Next, we used Transwell assay to investigate cell migration and invasion capacity. The results showed that the migration and invasion of CCLP1 and SG-231 cells transfected with the Twist1 siRNA were significantly decreased compared with the cells transfected with the si-control (Fig. 5D and E). We then investigated the effect of Twist1 on CCLP1 and SG-231 cell migration and invasion downregulated by miR-186. We found that Twist1 silencing could contribute to the inhibitory effect of miR-186 on CCLP1 and SG-231 cell migration and invasion (Fig. 5D and E).

DISCUSSION

Previous studies have indicated that miRNAs function as oncogenes or tumor suppressors to regulate the

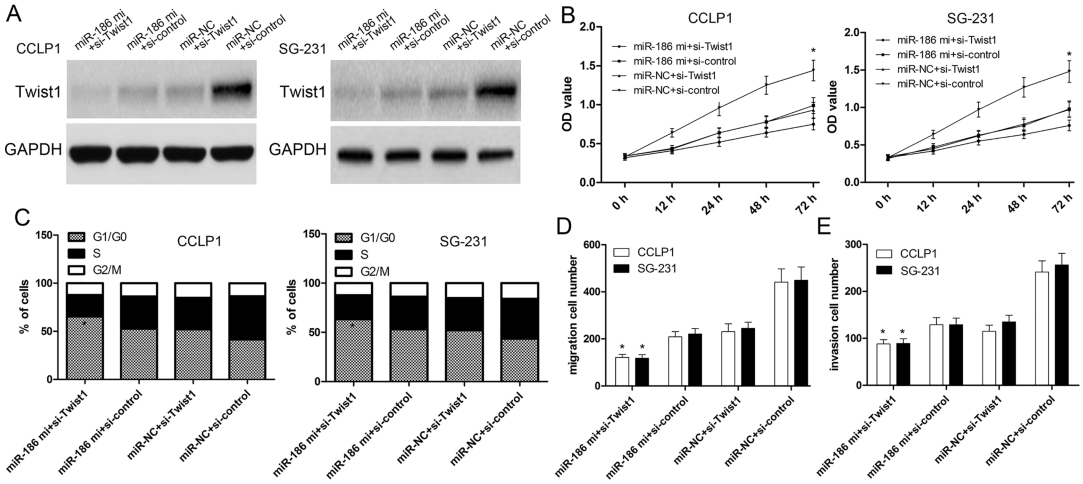

Figure 5. Twist1 is critical for the biological functions of miR-186 in CCA cells. (A) Western blot was performed to measure the relative expression of Twist1 protein. (B) Expression of Twist1 in CCLP1 and SG-231 cells after cotransfection of miR-186 mimics with si-control or si-Twist1. Then CCK-8 assay was performed to detect the cell proliferation ability. (C) Cell cycle was analyzed by flow cytometry at 72 h posttransfection. (D, E) Transwell assay was performed to determine the migration and invasion ability. Values presented as mean ± SD. *$p < 0.001$ versus control.

expression of cancer-associated genes[6,7]. Certain miRNAs have been demonstrated to be involved in the progression of CCA. Liu et al. reported that miR-494-dependent WDHDI inhibition suppresses EMT, tumor growth, and metastasis in CCA[11]. Sun et al. demonstrated that dysregulation of KCNQ1OT1 promotes CCA progression via miR-140-5p/SOX4 axis[12]. Zhou et al. suggested that miR-378 serves as a prognostic biomarker in CCA and promotes tumor proliferation, migration, and invasion[13]. In addition, Twist1 was also identified to play pivotal roles in tumor cell proliferation, cell growth, and metabolism[9,14,15]. For example, Liu et al. found that Twist1 promotes EMT and metastasis in lung adenocarcinoma[9]. More reports also indicated the role of Twist1 in regulating tumorigenesis and development[13,14]. Grither et al. indicated that Twist1 induces expression of discoidin domain receptor 2 to promote ovarian cancer metastasis[15]. Thus, Twist1 may serve as putative targets in the integral therapy of cancers. However, the relationship and interaction of miR-186 and Twist1 were not investigated in CCA.

In the present study, it was indicated that downregulation of miR-186 was identified in CCA tissues and cell lines, and negatively correlated with poor prognosis and the expression of Twist1. We then assumed that miR-186 exerted an important effect on the development of CCA. We found that overexpression of miR-186 affected cell proliferation and in vivo tumor formation, which was attributed to cell cycle arrest. Zhang et al. reported that miR-186 caused cell cycle arrest and inhibition of cell cycle-related proteins to inhibit proliferation and tumor formation in osteosarcoma[16]. Further, overexpression of miR-186 inhibited the expression of Twist1 and affected EMT progression of CCLP1 and SG-231 cells, thereby decreasing the migration and invasion capacity. In addition, silencing of Twist1 also resulted in cell cycle arrest, and affected proliferation of CCLP1 and SG-231 cells. Our results suggested that miR-186 may regulate the development of CCA probably by targeting Twist1.

miRNAs are primarily involved in the formation of the RNA silencing complex through incomplete base pairing with the 3′-UTR of target genes[17], leading to degradation or inhibition of protein translation of target genes[18–20]. Therefore, the target genes of miRNA are crucial to the function of miRNA in cancer cells[21,22]. In this study, bioinformatics analysis and luciferase assay confirmed that Twist1 is a direct target gene of miR-186, and silencing of Twist1 synergized the effects of miR-186 on the proliferation, cell cycle, migration, and invasiveness of CCA cells. Using bioinformatics, we also found no potential binding relationship among miR-186 and other EMT biomarkers (E-cadherin, N-cadherin, vimentin, and MMP9). Besides, Twist1 was reported to activate MMP2 expression via binding to its promoter in colorectal cancer[23]. Meng et al. unveiled a mechanism by which Twist1 regulates vimentin during EMT[24]. Lv et al. found that Twist1 regulates EMT via the NF-κB pathway in papillary thyroid carcinoma[25]. These results indicated that miR-186 targets Twist1 to regulate EMT.

In conclusion, miR-186 expression was decreased in CCA tissues and cell lines. Overexpression of miR-186 led to inhibition of cell proliferation, migration, and invasion of CCA cells by directly targeting Twist1. Thus, miR-186 is proposed to be a tumor suppressor and may

serve as a therapeutic target in the treatment of patients with CCA.

ACKNOWLEDGMENT: The authors declare no conflicts of interest.

REFERENCES

1. Labib PL, Goodchild G, Pereira SP. Molecular pathogenesis of cholangiocarcinoma. BMC Cancer 2019;19:185.
2. Auriemma F, De Luca L, Bianchetti M, Repici A, Mangiavillano B. Radiofrequency and malignant biliary strictures: An update. World J Gastrointest Endosc. 2019; 11:95–102.
3. Marya NB, Tabibian JH. Role of endoscopy in the management of primary sclerosing cholangitis. World J Gastrointest Endosc. 2019;11:84–94.
4. Simile MM, Bagella P, Vidili G, Spanu A, Manetti R, Seddaiu MA, Babudieri S, Madeddu G, Serra PA, Altana M, Paliogiannis P. Targeted therapies in cholangiocarcinoma: Emerging evidence from clinical trials. Medicina (Kaunas) 2019;55. pii: E42.
5. Lo Russo G, Tessari A, Capece M, Galli G, de Braud F, Garassino MC, Palmieri D. MicroRNAs for the diagnosis and management of malignant pleural mesothelioma: A literature review. Front Oncol. 2018;8:650.
6. Tian J, Shen R, Yan Y, Deng L. miR-186 promotes tumor growth in cutaneous squamous cell carcinoma by inhibiting apoptotic protease activating factor-1. Exp Ther Med. 2018;16:4010–8.
7. Cao Q, Wang Z, Wang Y, Liu F, Dong Y, Zhang W, Wang L, Ke Z. TBL1XR1 promotes migration and invasion in osteosarcoma cells and is negatively regulated by miR-186-5p. Am J Cancer Res. 2018;8:2481–93.
8. Lu K, Dong JL, Fan WJ. Twist1/2 activates MMP2 expression via binding to its promoter in colorectal cancer. Eur Rev Med Pharmacol Sci. 2018;22:8210–9.
9. Liu C, Luo J, Zhao YT, Wang ZY, Zhou J, Huang S, Huang JN, Long HX, Zhu B. TWIST1 upregulates miR-214 to promote epithelial-to-mesenchymal transition and metastasis in lung adenocarcinoma. Int J Mol Med. 2018;42:461–70.
10. Ji Q, Li Y, Zhao Q, Fan LQ, Tan BB, Zhang ZD, Zhao XF, Liu Y, Wang D, Jia N. KLF11 promotes gastric cancer invasion and migration by increasing Twist1 expression. Neoplasma 2019;66:92–100.
11. Liu B, Hu Y, Qin L, Peng XB, Huang YX. MicroRNA-494-dependent WDHDI inhibition suppresses epithelial-mesenchymal transition, tumor growth and metastasis in cholangiocarcinoma. Dig Liver Dis. 2019;51:397–411.
12. Sun H, Li Y, Kong H, Dai S, Qian H. Dysregulation of KCNQ1OT1 promotes cholangiocarcinoma progression via miR-140-5p/SOX4 axis. Arch Biochem Biophys. 2018; 658:7–15.
13. Zhou Z, Ma J. miR-378 serves as a prognostic biomarker in cholangiocarcinoma and promotes tumor proliferation, migration, and invasion. Cancer Biomark. 2019;24:173–81.
14. Funahashi S, Okazaki Y, Nagai H, Chew SH, Ogawa K, Toyoda T, Cho YM, Toyokuni S. Twist1 was detected in mesenchymal cells of mammary fibroadenoma and invasive components of breast carcinoma in rats. J Toxicol Pathol. 2019;32:19–26.
15. Grither WR, Divine LM, Meller EH, Wilke DJ, Desai RA, Loza AJ, Zhao P, Lohrey A, Longmore GD, Fuh KC. TWIST1 induces expression of discoidin domain receptor 2 to promote ovarian cancer metastasis. Oncogene 2018;37:1714–29.
16. Zhang Z, Zhang W, Mao J, Xu Z, Fan M. miR-186-5p functions as a tumor suppressor in human osteosarcoma by targeting FOXK1. Cell Physiol Biochem. 2019;52:553–64.
17. Vasilatou D, Papageorgiou S, Pappa V, Papageorgiou E, Dervenoulas J. The role of microRNAs in normal and malignant hematopoiesis. Eur J Haematol. 2010;84:1–16.
18. Wang QZ, Xu W, Habib N, Xu R. Potential uses of microRNA in lung cancer diagnosis, prognosis, and therapy. Curr Cancer Drug Targets 2009;9:572–94.
19. Okada H, Kohanbash G, Lotze MT. MicroRNAs in immune regulation—Opportunities for cancer immunotherapy. Int J Biochem Cell Biol. 2010;42:1256–61.
20. Cai B, Pan Z, Lu Y. The roles of microRNAs in heart diseases: A novel important regulator. Curr Med Chem. 2010;17:407–11.
21. Hummel R, Hussey DJ, Haier J. MicroRNAs: Predictors and modifiers of chemo- and radiotherapy in different tumour types. Eur J Cancer 2010;46:298–311.
22. Tsuchiya N, Nakagama H. MicroRNA, SND1, and alterations in translational regulation in colon carcinogenesis. Mutat Res. 2010;693:94–100.
23. Lu K, Dong JL, Fan WJ. Twist1/2 activates MMP2 expression via binding to its promoter in colorectal cancer. Eur Rev Med Pharmacol Sci. 2018;22:8210–9.
24. Meng J, Chen S, Han JX, Qian B, Wang XR, Zhong WL, Qin Y, Zhang H, Gao WF, Lei YY, Yang W, Yang L, Zhang C, Liu HJ, Liu YR, Zhou HG, Sun T, Yang C. Twist1 regulates vimentin through Cul2 circular RNA to promote EMT in hepatocellular carcinoma. Cancer Res. 2018; 78:4150–62.
25. Lv N, Shan Z, Gao Y, Guan H, Fan C, Wang H, Teng W. Twist1 regulates the epithelial-mesenchymal transition via the NF-κB pathway in papillary thyroid carcinoma. Endocrine 2016;51:469–77.